IAS-2008-AE0599

The 7th Iranian Aerospace Society Conference
Feb. 19-21/2008, Sharif University of Technology

Numerical study of the separation point for external flows

Mahmoud Passandideh-Fard[1], Mehran Mohammadi Farhangi[2], Amir Omidvar[3]
1-Asssistancd professor, fardmp@yahoo.com
2-Graduated student, farhangi.mehran@gmail.com
3- Graduated student, am.omidvar@gmail.com

Abstract
In this paper Numerical simulations are performed using the control volume method to obtain separation point of two-dimensional laminar, steady, incompressible flows. Low Reynolds number flows over cylinder, NACA 0012 and NACA 63_3-418 airfoil are considered under the influence of an external adverse pressure gradient for different attack angles in order to examine the accuracy of the experimental Stradford's criteria. Then the Stradford's criterion is amended accurately. Numerical results compared well with those of the Stratford's criteria for NACA 63_3-418, NACA 0012 airfoil and cylinder.

Keywords: *Stradford- separation point- air foil*

Introduction

The studies of external flows around bodies are of great importance in many engineering fields. In these cases predicting the separation is of particular interest. It occurs when the main stream separates from the surface of the body, and causes a large drag. In the design of bodies' shapes certain measures should be taken to prevent separation by using streamlined contours and boundary-layer control techniques.

A laminar boundary layer over a solid surface will separate as a result of curvature changes or adverse pressure gradient. Obviously, the length of the separation bubble depends on the location of transition. On the other hand, the size of the separation bubble could directly affect the flight characteristics of the airfoil and the efficiency of the turbo machine. The flow separation over a wing in flight results in the loss of lift and the increase of drag as well as the generation of aerodynamic noise and it also reduces the stability and efficiency of the aircraft. Understanding the mechanism of the separation and transition is of great importance in improving the design of aircrafts and turbo-machines.

With separated flows, the separation zone is complex and the characteristics of a separation structure may depend on whether the boundary layer is laminar or turbulent upstream of separation. To understand the basic characteristics of boundary layer separation, many investigators have studied two-dimensional, steady, laminar separation [2].

The typical structure of a laminar boundary layer separation was achieved experimentally by Stradford.

$$\overline{c_p}\left(\overline{x}\frac{d\overline{c_p}}{dx}\right)^2 = 0.0104 \tag{1}$$

$$\overline{x_m} = \int_0^{x_m}\left(\frac{u_e}{u_m}\right)^5 dx \tag{2}$$

$$\overline{x} - \overline{x_m} = x - x_m \tag{3}$$

$$\frac{q_t}{q_m} = 1 - \overline{c_p} \tag{4}$$

Where $\overline{x_m}$ and other parameters used in Stradford's criteria are shown in Fig. 1.

[1] Assistance professor, fardmp@yahoo.com
[2] Graduated student, farhangi.mehran@gmail.com
[3] Graduated student, am.omidvar@gmail.com

Numerical Method

First the fluid domain is divided into a large number of discrete control volumes (also known as cells). Once the fluid domain has been descretized, the governing equations (in integral form) for the conservation of mass, momentum, energy and any other relevant variable are applied to each discrete control volume and used to construct a set of non-linear algebraic equations for the discrete dependent variables. The complete set of coupled equations for all the control volumes is then solved using either a segregated or coupled solver. In this paper only the segregated solver has been used. Since the flow before the separation point is laminar, the Stradford's criteria is used to obtain the inception of separation over airfoil. In order to get the best results, simulations were conducted using the turbulence models: renormalizable k-ε, Reynolds stress, Spalart-Allmaras and k-ω, since the flow after the separation point is turbulent. The results of the two last turbulence models mentioned above were very close to each other. Thus the Spallart-Allmaras model is used for airfoils to reduce the computational time and for cylinder unsteady laminar model is used. The Spalart-Allmaras model [3] is a relatively simple one-equation model that solves one modeled transport equation for the kinematic eddy (turbulent) viscosity.

The Spalart-Allmaras model was designed specifically for aerospace applications involving wall-bounded flows and has been shown to give good results for boundary layers subjected to adverse pressure gradients. In its original form, the Spalart-Allmaras model is effectively a low-Reynolds-number turbulence model, requiring the viscous-affected region of the boundary layer to be properly resolved.

The Spalart and Allmaras model belongs to the family of eddy viscosity models. This family of models is based on the assumption that the Reynolds stress tensor ($-\overline{\rho u_i u_j}$) is related to the mean strain rate through an apparent turbulent viscosity called eddy viscosity υ_T

$$-\overline{u_i u_j} = \upsilon_T \left(\frac{\partial \overline{u_i}}{\partial y^i} + \frac{\partial \overline{u_j}}{\partial y^i}\right) \tag{2}$$

In the Spalart and Allmaras model, the eddy viscosity is computed through a partial differential equation. In particular the eddy viscosity υ_T is computed by an intermediate variable $\tilde{\upsilon}$ through the relation

$$\upsilon_T = \tilde{\upsilon} f_{\upsilon 1}(\chi) \tag{3}$$

Where χ is the ratio

$$\chi = \frac{\tilde{\upsilon}}{\upsilon} \tag{4}$$

And $f_{\upsilon 1}$ is a damping function. The intermediate variable $\tilde{\upsilon}$ is computed by solving a differential equation that can be written in compact form as in a fixed point. It should be pointed out that, although the transition onset point has to be user-specified, the flow development in the transition region is built into the model through this trip source term. The quantities enclosed between the brackets show the main depending variables of these source terms. In particular S denotes the vorticity magnitude, d the wall distance and dT the distance from the transition point. The last term in the right hand side is a diffusion term in which σ and cb2

$$\begin{aligned} \frac{D\tilde{\upsilon}}{Dt} &= b_{prod}(S, \tilde{\upsilon}, d) \\ &- b_{dest}(\tilde{\upsilon}, d) + b_{trip}(d_T) \\ &+ \frac{1}{\sigma}\left[\nabla.((\upsilon + \tilde{\upsilon})) + c_{b2}(\nabla \tilde{\upsilon})^2\right] \end{aligned} \tag{3}$$

Where the symbols b_{prod} and b_{dest} indicate respectively the production term and the destruction term and finally b_{trip} denotes a special source term which allows the laminar-turbulent transition in a fixed point. It should be pointed out that, although the transition onset point has to be user-specified, the flow development in the transition region is built into the model through this trip source term. The quantities enclosed between the brackets show the main depending variables of these source terms. In particular S denotes the vorticity magnitude, d the wall distance and dT the distance from the transition point. The last term in the right hand side is a diffusion term in which σ and cb2 denote respectively the turbulent Prandtl number and a calibration constant.

Results

The primary goal of this research is to compare the Stratford's predictions with numerical result. The numerical results are also validated with experimental data by Abbot [1]**.**

In order to obtain the separation point from the numerical solutions, the velocity vector is followed along the surface of the airfoil. The separation point is considered where the velocity vector of the adjacent point to the wall was equal to zero or reversed initially**.** In order to find the maximum velocity in each cross section of the flow, the sections were made for a constant step size of (0.005m) on airfoil surface. This amount of velocity is used for Eq. (4). The separation point(x) is achieved by Eq. (1).

As a first step, the separation point was obtained for different attack angles at low Reynolds numbers (Re<1 million & M<1) for NACA 63_3-418 and NACA 0012 and compared with Stradford's criteria which is shown in Fig.2 and Fig.3. Numerical simulation results, shown by the solid line, appear to describe well the separation point. As seen from this figures, increasing the attack angles decrease the separation point for both of numerical results and stradford's criteria. The numerical results match well with the theoretical one.

Velocity contours obtained for two airfoils and cylinder are given in Fig. 3, 4 and 5.

To obtain von-Karman vortex street and separation point below 90˚ for cylinder it was solved as unsteady

problem which is checked by stradford's criteria when it was periodically converged (300 second after uniform symmetric initial condition) and results shown only 7% error.

Table 1 – Separation point for cylinder

	X(m)
Separation point by numerical solution	0.593
Separation point by stradford's criteria	0.5497

Conclusion

The comparison between the numerical results with Sradford's criteria to obtain the separation point shows that numerically computed ones agree well with experimental ones in high attack angles. Also results for unsteady periodic cylinder shows very well agreement.

References

1- I. H. Abbot, A. E. Von Doenhoff, " Theory of wing sections ", Dover publications, New York, 1959.

2- J.C. Muti Lin and Laura L. Pauley. Low -Reynolds number separation on an airfoil. AIAA J., 34:8-12, 1996

3- R. Paciorri, W. Dieudonne', G. Degrez, J.-M Charbonnier, and H. Deconinck, " Validation of the Spallart-Allmaras Turbulence model for Application in hypersonic flows "Appl 97-2023,AIAA Fluid Dynamics Conference, June 29-july 2, Snowmass Village, Collarado (1997)

Figures

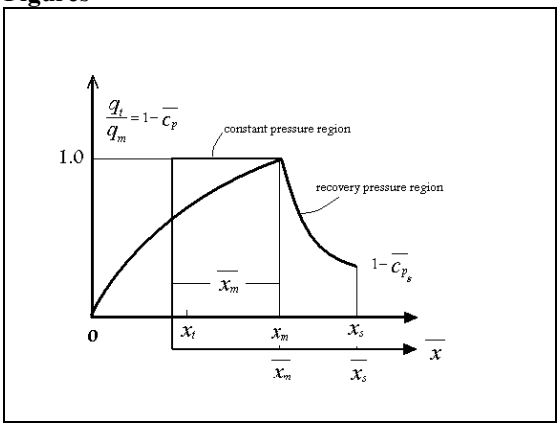

Fig. 1 Stradford's parameter

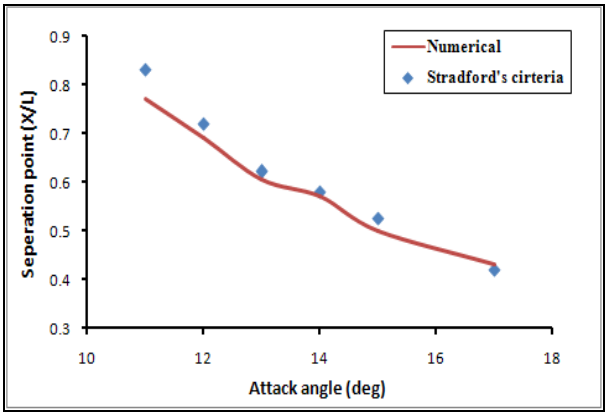

Fig. 2 Comparison of simulated and experimental values of separation point versus attack angle for NACA 63_3-418.

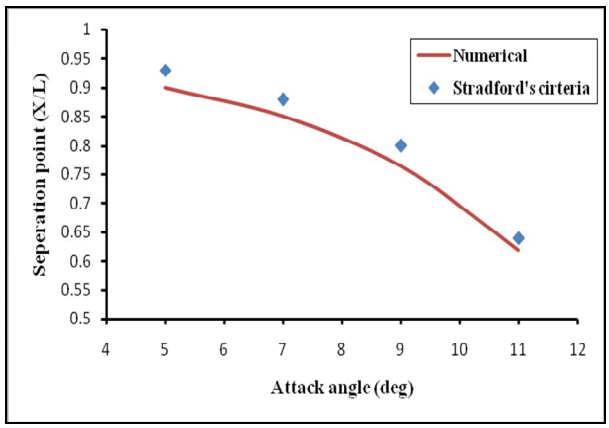

Fig. 3 Comparison of simulated and experimental values of separation point versus attack angle for NACA 0012.

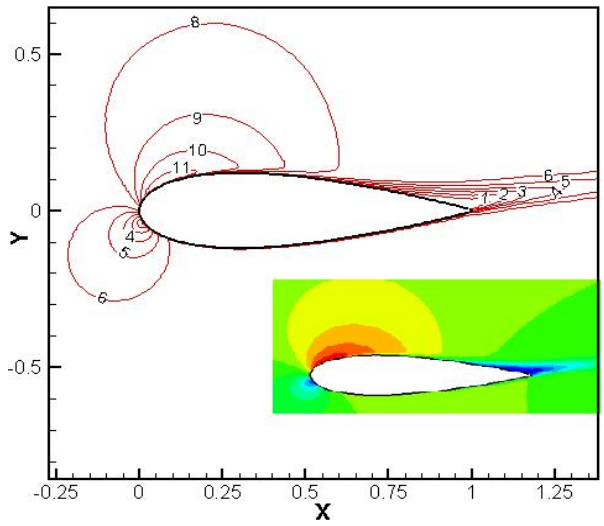

Fig. 4 Velocity contour for NACA 0012 at α=9°

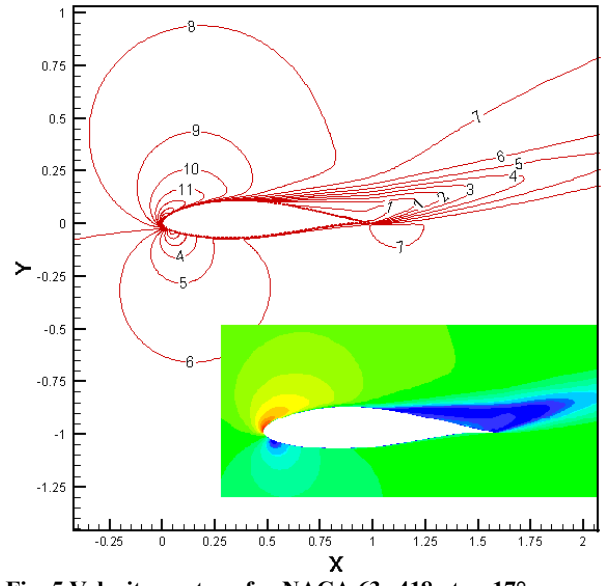

Fig. 5 Velocity contour for NACA 63_3-418 at α=17°

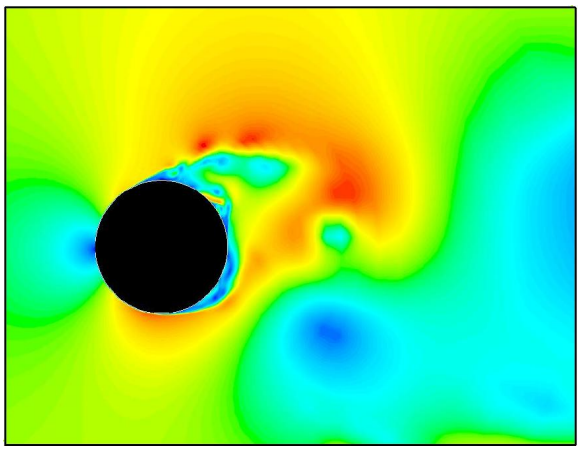

Fig. 6 Unsteady velocity contour for cylinder at time=300 second